Decarburization of Stainless Steel: Part I. A Mathematical Model for Laboratory Scale Results

SHIGEO ASAI AND JULIAN SZEKELY

A mathematical model is presented for describing the reaction of iron-chromium-carbon melts with pure oxygen, air and oxygen-argon mixtures. The model is based on the generalization of the Asai-Muchi model for oxygen steelmaking to systems containing chromium and where the oxygen blown is diluted by an inert gas. The predictions based on the model were compared to the experimental measurements of Barnhardt obtained with heats of about 1.2 to 1.5 kg, having carbon contents ranging from 0.3 to 0.6 wt pct and chromium contents of 0.0 to 21.0 wt pct. The agreement between measurements and predictions was quite good for a variety of blowing arrangements which included top blowing with pure oxygen or air and bottom blowing with air. The fact that this good agreement was obtained by using a single value of the adjustable parameter in the model for all runs, renders very promising the extension of the model to more complicated systems.

IN recent years there has been a growing interest in the application of new processes, such as the U.C.C. (O_2-Ar)[1] and the Witten Process,[2] as alternatives to the electric furnace for the refining of stainless steel.

The principal objective of these processes is to obtain very low carbon levels by selective oxidation, while achieving good chromium recovery.

In order to provide improved process control and to devise the optimum operating conditions for these systems it would be desirable to obtain suitable mathematical models for these operations. However, a good quantitative understanding of the kinetics of the decarburization of Cr-C-Fe alloys, which would be a necessary prerequisite for the construction of mathematical models for these processes, is not available at the present.

While numerous interesting laboratory scale measurements have been reported in the literature on the surface decarburization of Cr-C-Fe alloys[3,4,5,6] the actual interpretation of these kinetic data is not really suitable for process modeling purposes.

The work to be described in this paper was undertaken as part of a continuing effort aimed at the mathematical modeling and optimization of stainless steel decarburization processes. Part I of the series is concerned with the adaptation of a previously published "Unified Model for Steelmaking Processes" to the interpretation of laboratory scale measurements. The subsequent Part II will be devoted to the modeling of pilot scale and plant scale operations.

Regarding the organization of the paper, in the following Section I we shall present a brief review of the "Unified Model for Steelmaking Processes;" the development of the actual model dealing with stainless steel operations is given in Section II, the computed results are given in Section III. Finally, the concluding remarks are contained in Section IV.

SHIGEO ASAI is Postdoctoral Fellow, Center for Process Metallurgy at the State University of New York at Buffalo, on leave from Department of Iron and Steel Engineering, Nagoya University, Nagoya, Japan. JULIAN SZEKELY is Professor Chemical Engineering and Director of the Center for Process Metallurgy, State University of New York at Buffalo, Buffalo, New York 14214.

Manuscript submitted August 13, 1973.

I. THE UNIFIED MODEL OF OXYGEN STEELMAKING PROCESSES

In the development of a unified model for oxygen steelmaking processes Asai and Muchi[7,8,9] proposed that during the oxygen blow the concentration of each alloying element in the bath may be calculated by establishing a balance between two driving forces, namely:

a) driving force which will cause the system to tend towards thermodynamic equilibrium

b) another driving force, due to the oxygen supplied to the bath, which will tend to keep the system from reaching equilibrium.

In order to illustrate this concept, let us consider a time period toward the end of the blow, where we may consider the oxidation of carbon as a sole reaction, thus the oxygen supplied to the metal is either used for decarburization, or it accumulates in the metal phase.

Upon considering (plant and laboratory scale) experimental data for the relationship between the oxygen and carbon content of the bath, it has been established that the concentration of these bath components is in excess of the equilibrium values.[10,11] This is illustrated in Fig. 1(a), where the solid line represents the equilibrium relationship, between the dissolved carbon and oxygen, whereas the broken line corresponds to the actual decarburization trajectory.

We may now proceed by establishing an oxygen balance over a time period Θ, which may be written as:

$$\int_0^{\Theta} (S/W)\, d\Theta = (C_o - C_{i,o}) + (M_o/M_c)(C_{i,c} - C_c) \quad [1]$$

where W and S are the mass of the melt and the feed rate of the available oxygen, respectively; M_c and M_o denote the molecular weights of carbon and oxygen, respectively, C_c and C_o denote the carbon and oxygen concentrations in the melt while the additional subscript i refers to the initial values.

The behavior of the system may now be represented by a series of operating lines, also shown in Fig. 1(a), which have the following physical significance:

If the supply of oxygen were suddenly cut when the composition of the system was at point J, then the

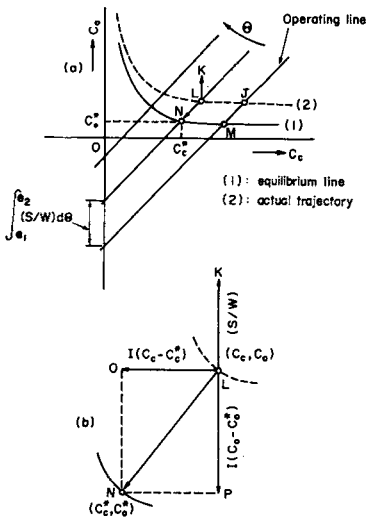

Fig. 1—(*a*) The equilibrium relationship and the "operating lines" for the iron-carbon-oxygen system. (*b*) Magnified version of the region *L*-*N*.

composition of the melt would move along the line drawn through *J* until equilibrium is reached at point *M*. As the blow proceeds the behavior of the system would be represented by the parallel displacement of the original operating line, in the direction of the arrow, as shown in the graph.

For given bath carbon and oxygen concentrations (or rather activities) the corresponding equilibrium values will depend on the temperature and on the CO partial pressure only, thus this relationship may be expressed as:

$$C_o \cdot C_c = P_{CO}/K(T) \qquad [2]$$

It follows, that with the aid of Eqs. [1] and [2], we may calculate the equilibrium composition of the bath that would correspond to the concentration levels in the bath, attained after the lapse of a given time period, Θ.

Let us now consider the situation where the bath composition corresponds to the point *L*; then the intersection of the operating line and the equilibrium line is given by a point *N*, thus the system would move from the point *L*, to the point *N* due to the driving force, $\overrightarrow{LN}$. Fig. 1(*b*) is the magnificed version of Fig. 1(*a*), where it is shown that the driving force, $\overrightarrow{LN}$ can be resolved into the two components, $\overrightarrow{LO}$ and $\overrightarrow{LP}$.

Let us now consider the effect of oxygen transfer into the metal. As oxygen is being transferred into the metal, for a system originally at point *L*, there is a driving force acting on the system in the direction $\overrightarrow{LK}$, as seen in Fig. 1. In assessing the rate at which the system will move due to these driving forces, let us designate the *conductances* or reciprocal resistances of the system by *I*, also shown in the graph. These quantities, *I*, are considered to incorporate all the resistances to transfer, *i.e.*, mass transfer, chemical kinetics, mixing, etc.; the way in which this is done will be discussed subsequently.*

*Strictly speaking, the resistances associated with the transfer of oxygen and carbon should be different but experience has shown[7,8,9] that the same value of *I* may be used for all the bath components.

We may now proceed by using these conductance terms to express conservation of oxygen and carbon in the following differential forms:

$$dC_o/d\Theta = I(C_o^* - C_o) + S/W \qquad [3]$$

$$dC_c/d\Theta = I(C_c^* - C_c) \qquad [4]$$

In a geometric sense the derivatives appearing in Eqs. [3] and [4] correspond to the displacement of the point *L* by an infinitesimal distance along the broken line.

The above considerations may be readily generalized to ternary or multi-component systems. The behavior of a ternary system, components of which in the present case are carbon, chromium and oxygen, is sketched in Fig. 2. Here the axes, *X*, *Y*, and *Z* represent the concentrations of carbon, chromium and oxygen, respectively. The equilibrium lines *X*-*Z* and *Y*-*Z* are illustrated on the *X*-*Z* and *Y*-*Z* planes, respectively; the intersection of these curved surfaces represents the equilibrium relationship for a three component system.

On the analogy of Eq. [1] for the binary system, the conservation of oxygen for the ternary system considered here may be written as:

$$\int_o^{\Theta} (S/W)\,d\Theta = (C_o - C_{i,o}) + (M_o/M_c)(C_{i,c} - C_c) + \tfrac{3}{2}(M_o/M_{cr})(C_{i,cr} - C_{cr}) \qquad [5]$$

As shown in Fig. 2, Eq. [5] represents the *operating plane which moves* in the direction given by the arrow during the progress of the blow. We note that Eq. [5] may be written in a more general form for multi-component systems to obtain:

$$\int_o^{\Theta} (S/W)\,d\Theta = \sum_{j=1}^{n} \alpha_j (M_o/M_j)(C_{i,j} - C_j) \qquad [6]$$

where $j = 1, 2, \ldots n$, and α_j is a stoichiometric coefficient.

On the analogy of the binary case we may make use of the concept of the conductances and write the differential oxygen and component balances, which take the following form:

$$dC_o/d\Theta = I(C_o^* - C_o) + S/W \qquad [7]$$

$$dC_j/d\Theta = I(C_j^* - C_j),\ j = 2 \sim n \qquad [8]$$

The equilibrium concentrations C_o^* and C_j^* appearing

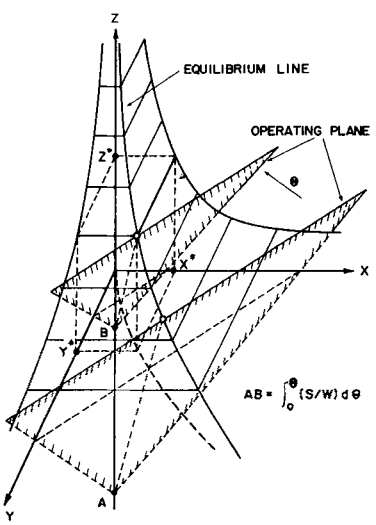

Fig. 2—Schematic diagram of the equilibrium line and of the operating planes in rectangular coordinates.

in Eqs. [7] and [8] will depend on the partial pressure of CO above the bath, the bath temperature and in general, on the bath composition.

This technique has been used for predicting bath composition trajectories for oxygen steelmaking on both industrial and laboratory-scale systems. The purpose of the present paper is to extend the application of the method of the decarburization of ferrochrome.

II. STATEMENT OF THE PROBLEM

Let us consider a system where a molten chromium-carbon-iron alloy is made to react with pure or diluted oxygen. The treatment will be general so that we shall be able to consider both top blowing and bottom blowing arrangements. Let us assume, furthermore, that the principal reaction products are CO and Cr_2O_3; while the model does not allow for the formation of FeO explicitly, C_o the oxygen concentration is deemed to include the available oxygen both in the bath and in the slag. It is realized that this is an oversimplification, which among other assumptions postulates that the oxygen transfer from the FeO part of the slag to the metal is quite rapid.

Under these conditions the principal reactions may be written as:

$$\underline{C} + \underline{O} \rightleftarrows CO(g) \quad [9]$$

$$2\underline{Cr} + 3\underline{O} \rightleftarrows Cr_2O_3(S) \quad [10]$$

The pertinent equilibrium relationships may be expressed as:

$$K_1 = P_{CO}/a_C \cdot a_O \quad [11]$$

$$\log K_1 = 1017/T + 2.14 \quad \text{(Ref. 12)} \quad [12]$$

$$K_2 = a_{Cr_2O_3}/a_{Cr}^2 a_O^3 \quad [13]$$

$$\log K_2 = 44040/T - 19.42 \quad \text{(Ref. 12)} \quad [14]$$

It is noted here that for the purpose of calculation we have assumed that $a_{Cr_2O_3} = 1$; as will be shown subsequently the equilibrium concentrations of oxygen, chromium and carbon in the melt may be calculated for various values of P_{CO}. The partial pressure of CO above the melt is not immediately available at this stage, but has to be calculated through the use of a trial and error procedure. The interaction coefficients are given by:

$$e_O^{Cr} = -158/T + 0.038 \quad \text{(Ref. 12)} \quad [15]$$

$$e_C^C = 358/T \quad \text{(Ref. 13)} \quad [16]$$

$$e_C^{Cr} = -0.023 \quad \text{(Ref. 12)} \quad [17]$$

$$e_{Cr}^C = (M_{Cr}/M_C) \cdot e_C^{Cr} + \tfrac{1}{230}(M_C - M_{Cr})/M_C \quad [18]$$

Most of these thermodynamic data are quoted from the work of Nakamura et al.,[12] obtained for Cr contents of 10 pct to about 25 pct and over the temperature range, 1600°C to 1900°C. These experimental conditions correspond quite closely to the conditions encountered in stainless steelmaking processes.

By using these interaction coefficients the activity coefficients f of oxygen, carbon and chromium may be expressed as:

$$\log f_O = e_O^{Cr} \cdot C_{Cr} \quad [19]$$

$$\log f_C = e_C^{Cr} \cdot C_{Cr} + e_C^C \cdot C_C \quad [20]$$

$$\log f_{Cr} = e_{Cr}^C \cdot C_C \quad [21]$$

Through the use of these activity coefficients the equilibrium relationships may then be written in terms of concentrations which are necessary in the mass balance calculations. We may now proceed by restating the previously derived conservation equations.

Thus the oxygen balance is written as:

$$\int_o^\Theta (S/W)\, d\Theta = (C_o - C_{i,o}) + (M_o/M_C)(C_{i,C} - C_C) + \tfrac{3}{2}(M_o/M_{Cr})(C_{i,Cr} - C_{Cr}) \quad [5]$$

Furthermore, the differential oxygen, carbon and chromium balances may be written as:

$$dC_o/d\Theta = I(C_o^* - C_o) + (S/W) \quad [7]$$

$$dC_C/d\Theta = I(C_C^* - C_C) \quad [22]$$

$$dC_{Cr}/d\Theta = I(C_{Cr}^* - C_{Cr}) \quad [23]$$

Eqs. [7], [22] and [23] may be put in the following dimensionless form:

$$dc_o/d\theta = A(c_o^* - c_o) + B \quad [24]$$

$$dc_C/d\theta = A(c_C^* - c_C) \quad [25]$$

$$dc_{Cr}/d\theta = A(c_{Cr}^* - c_{Cr}) \quad [26]$$

where, $A \equiv I\Theta_s$, $B \equiv S\Theta_s/WC_s$, $c_j \equiv C_j/C_s$, $\theta \equiv \Theta/\Theta_s$.

The partial pressure of carbon monoxide gas used in Eq. [11] is obtained by establishing a mass balance at the gas metal interface:

$$P_{CO} = \frac{N_{CO}}{N_{O_2} + \tfrac{1}{2}N_{CO} + N_g - N_{O_2,Cr}} \times P_t = \frac{M_C N_{CO}}{\lambda S/W + \tfrac{1}{2}M_C N_{CO} - M_C N_{O_2,Cr}} \times P_t \quad [27]$$

where the coefficient, $\lambda = (M_C/M_{O_2})[1 + (N_g/N_{O_2})]$, is evaluated from the flow rates of the oxygen and of the carrier gas, N_g which are obtained from the experimental conditions. The rates at which carbon monoxide is released and oxygen is consumed are related to the rate of change of the bath composition in the following manner:

$$N_{CO} = (dc_C/d\theta)(C_s/\Theta_s)/M_C \quad [28]$$

$$N_{O_2,Cr} = \tfrac{3}{4}(dc_{Cr}/d\theta)(C_s/\Theta_s)/M_{Cr} \quad [29]$$

The equilibrium concentrations, c_o^*, c_C^*, and c_{Cr}^* in Eqs. [24] to [26] are obtained by solving Eqs. [5], [11], [13], [15] to [20] and [21] simultaneously. However, the partial pressures of carbon monoxide gas appearing in Eq. [11] cannot be evaluated without solving Eqs. [24] to [26]. This means that an iterative procedure must be used for determining the value of p_{CO} and the time derivatives of the concentrations. The actual computational procedure is described in the next section.

III. COMPUTATION AND RESULTS

3.1 The Method of Solution

The procedure adopted for the solution required, that for known oxygen and carrier gas flow rates and for a given bath composition, the new bath composition be calculated after a given time step.

1) In advancing the solution by one time step the partial pressure of the carbon monoxide was assumed and the equilibrium concentrations of chromium, carbon and oxygen (c^*_{Cr}, c^*_C and c^*_O) were calculated with the aid of Eqs. [5] and [11] to [21].

2) Then by substituting the equilibrium concentrations thus obtained into Eqs. [24] to [26] and by using Eqs. [27] to [29] a new estimate is obtained for P_{CO}.

3) If the value of P_{CO} thus obtained was within 0.005 atm of the previous estimate, the solution was advanced by one time step using Eqs. [24] to [26] to calculate the new bath composition.

4) If this convergence criterion was not met the iterative procedure was repeated until satisfactory agreement was obtained. The actual computer flow chart employed in the calculations is given in the Appendix where some further comments are also made on the computational procedure.

3.2 Comparison of the Computed Results with Measurements

In order to examine the appropriateness of the model Figs. 3 to 10 show a set of the computed results which are compared with the experimental measurements of L. F. Barnhardt,[4] obtained with induction stirred heats about 1200 to 1500 g in weight. It is noted that a fixed value of the conductance parameter A was assumed in all these calculations, such that $A = 5$, for $\Theta = 3600$ s. The same value was used for all four types of experiments considered, namely:

1) Reaction of the melt with pure oxygen.

2) Reaction of the melt with oxygen, with the furnace atmosphere diluted with argon.

3) Reaction of the melt with air blow from the top.

4) Reaction of the melt with air blown from the bottom.

i) SYSTEMS TOP-BLOWN WITH OXYGEN

Figs. 3 and 4 show the behavior of systems where the melt was reacted with pure oxygen, blown at rates of 120,200 and 250 ml/min (STP) onto the top of the melt.

Fig. 3 shows the composition trajectories followed by the melt, on a plot of bath carbon against bath chromium at a temperature of 1600°C. The solid lines represent the predictions based on the model and the equilibrium relationship is also shown (with a broken line) for the purpose of comparison. It is seen that, in general, there is reasonably good agreement between measurements and predictions. In the initial stages only carbon is being oxidized but toward the end of the run substantial oxidation of chromium occurs. It is noted that the final carbon concentrations are seen to fall below the equilibrium line, calculated for one atmosphere CO pressure. This behavior may be explained by the fact that P_{CO}, as calculated from Eq. [27] has a value lower than unit under these conditions.*

*In calculating P_{CO}, we have to use $\lambda = 0.375$ since pure oxygen is being used, *i.e.*, there is no carrier gas.

Fig. 4 shows a plot of the chromium and carbon trajectories for the same runs given in the previous graph. It is seen that there is good, quantitative agreement between the measured and the predicted trajectories and

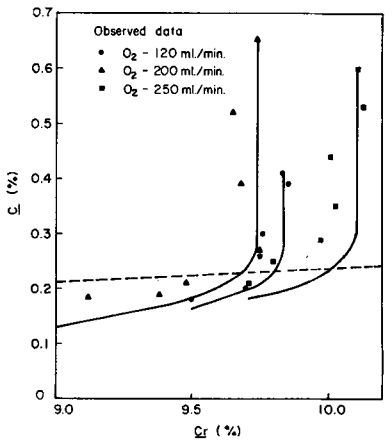

Fig. 3—A comparison of predictions and measurements for a top blown system, on a plot of carbon vs. chromium, using Barnhardt's data.[4] The solid lines represent the predictions, while the circles, rectangles and triangles represent the experimental measurements.

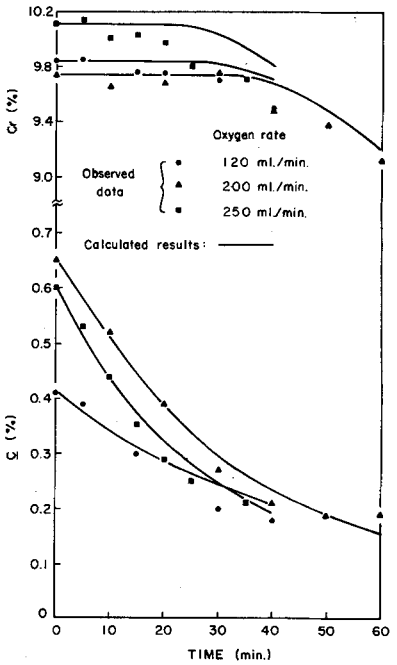

Fig. 4—Comparison of measurements and predictions for a top blow system, showing chromium and carbon trajectories, using Barnhardt's experimental data.

it may be worthwhile to reiterate that the same value of A was used in all the runs, notwithstanding the different flow rate employed.

ii) SYSTEMS TOP-BLOWN WITH OXYGEN, WHILE THE FURNACE ATMOSPHERE IS DILUTED WITH ARGON

Figs. 5 and 6 show both experimental data and predictions for the behavior of a system which was top blown by oxygen but where the furnace atmosphere was diluted with a continuous argon stream. As the flow rate of the argon was not given in Ref. 4, the values of $\lambda = 0.5$ and 1.5 were assumed in the computation of Fig. 5, whereas λ was assumed to be 1.5 in the computation of Fig. 6.

Inspection of Fig. 5 shows that the experimental data

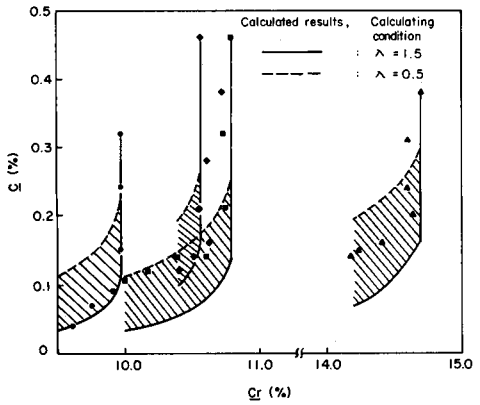

Fig. 5—Comparison of predictions and measurements for a top blown system, but where the furnace atmosphere was diluted with argon, using Barnhardt's results.[4] The solid lines represent the theoretical predictions and the data points correspond to the following oxygen flow rates: ●▲ 100 ml./min; ■ 150 ml./min; ◆ 225 ml./min.

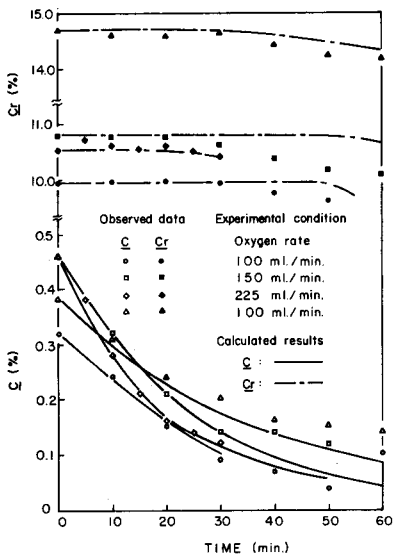

Fig. 6—Comparison of experimental measurements[4] and computed chromium and carbon trajectories for the same system as given in Fig. 5.

are again quite satisfactorily represented by the model provided $0.5 \leq \lambda \leq 1.5$ which corresponds to the shaded area. If one wished to treat λ as an adjustable parameter one could have obtained an even better agreement, but this would not have served any useful purpose, because in general the value of λ should be known.

Fig. 6 shows the chromium and the carbon trajectories for the same set of data presented in the previous graph and here again, there appears to be good quantitative agreement between measurements and predictions based on the model.

iii) SYSTEMS TOP-BLOWN WITH AIR

Figs. 7 and 8 show a comparison of experimental measurements and predictions based on the model for systems top blown with air at a rate of 300 ml/min (STP). Inspection of these graphs indicates reasonably good agreement between predictions and measurements on both the chromium vs carbon plots and the chromium and carbon trajectories depicted in Figs. 7 and 8, respectively.

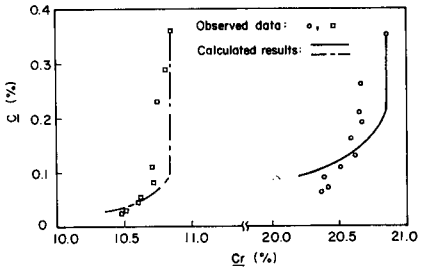

Fig. 7—Comparison of measurements[4] and predictions for a system top blown with air. The solid lines represent the theoretical predictions, the data points correspond to an airflow rate of 300 ml./min.

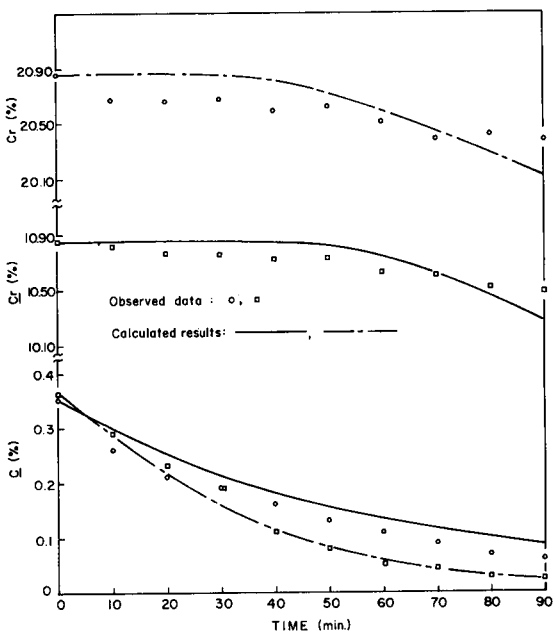

Fig. 8—The behavior of the top blown system, described in Fig. 7, now shown by plotting the chromium and the carbon trajectories.

iv) SYSTEMS BOTTOM-BLOWN WITH AIR

Finally, Figs. 9 and 10 show both measurements and predictions for a system where air was bubbled through the melt at a rate of 300 ml/min (STP) by using an alumina tube.

The carbon vs chromium trajectories are presented in Fig. 9 for three different initial concentrations and it is seen that the agreement between measurements and predictions is quite good.

Fig. 10 shows plots of the chromium and the carbon trajectories for the same runs; however, this plot also includes a decarburization run—with no chromium present. As perhaps expected, the agreement between measurements and predictions is excellent for this two-component system but the predictions appear to be quite reasonable for the other runs as well.

IV. CONCLUDING REMARKS

In the paper a previously developed model for oxygen steelmaking has been adapted for describing the oxidation trajectories of iron-carbon-chromium alloys.

In order to test the model, the predicted trajectories were compared with experimental measurements re-

ported by Barnhardt for a laboratory scale system. These measurements were made with heats of about 1200 to 1500 g, over a carbon concentration of 0.30 to 0.65 pct and a chrome concentration of 0 to 21 pct. The actual experimental arrangement included the jetting of pure oxygen and air onto the melt surface, the use of argon as a diluent for the furnace atmosphere and the bottom blowing of air.

It was found that the chromium and carbon trajectories could be quantitatively predicted for all these runs using a fixed value of the adjustable parameter A in the model.

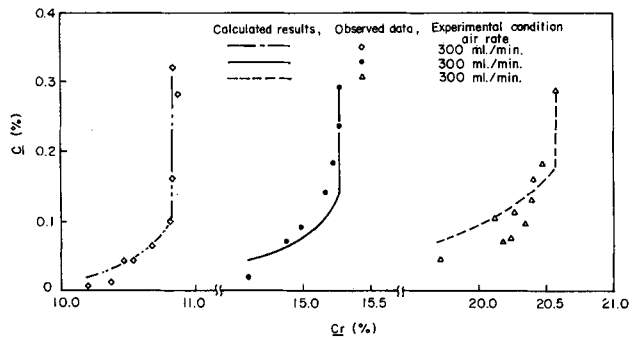

Fig. 9—Comparison of measurements[4] and predictions for a system bottom blown with air, on a plot of chromium vs. carbon.

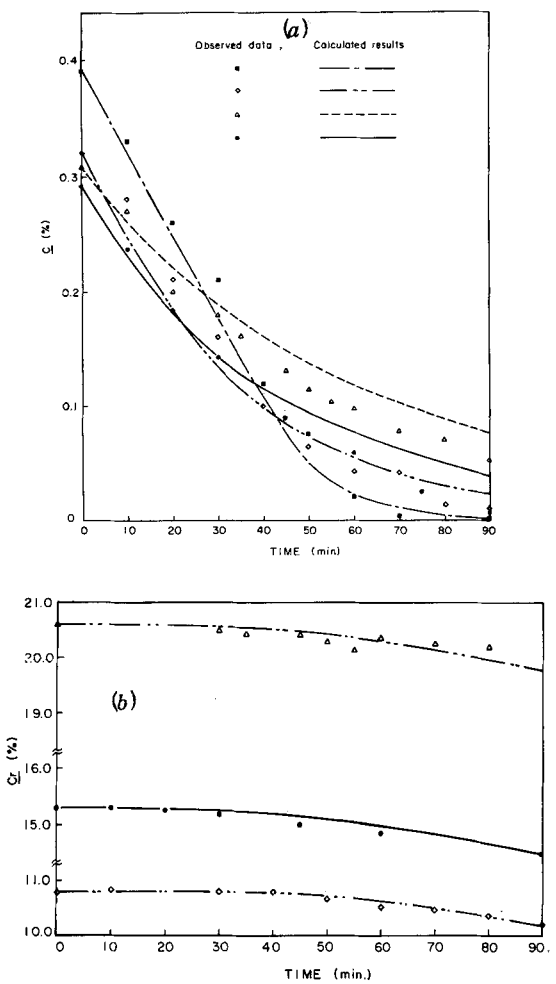

Fig. 10—Comparison of measurements[4] and predictions for a system bottom blown with air. (*a*) the carbon trajectory; (*b*) the chromium trajectory.

It is realized that the experimental conditions in the laboratory-scale study modeled were considerably simpler than those to be encountered in real stainless steelmaking operations, where the principal complicating factors would be caused by: non-isothermal conditions, more complex slags, possible bath inhomogeneities.

It is thought, nonetheless, that the technique shows promise for the modeling of these more complex industrial systems and work is currently in progress in this area.

APPENDIX

Estimation of the CO Partial Pressure Above the Bath

As described in the paper the concentration and temperature trajectories during the refining period were obtained by the simultaneous solution of Eqs. [5], [11] to [21] and [24] to [29]. Ordinarily the numerical solution of simultaneous, ordinary, differential equations would pose no special problem, however, some difficulties could have been encountered in the present case in the calculation of the partial pressure of CO above the bath. The system of equations are very sensitive to P_{CO} so that inaccuracies in the calculation of this quantity could have led to instability.

In order to circumvent this problem the following procedure was used for estimating P_{CO}, the flow chart of which is illustrated in Fig. A1:

The actual computation proceeded according to the following sequence:

1) An initial estimate was made of P_{CO} by forming the mean of the upper and lower limits assigned to this quantity.

2) By using this value of P_{CO}, through a series of intermediate calculations a second estimate was obtained for the partial pressure of carbon monoxide above the bath.

3) If this second estimate of P'_{CO} was found to be within 0.005 atm of the first estimate, which would

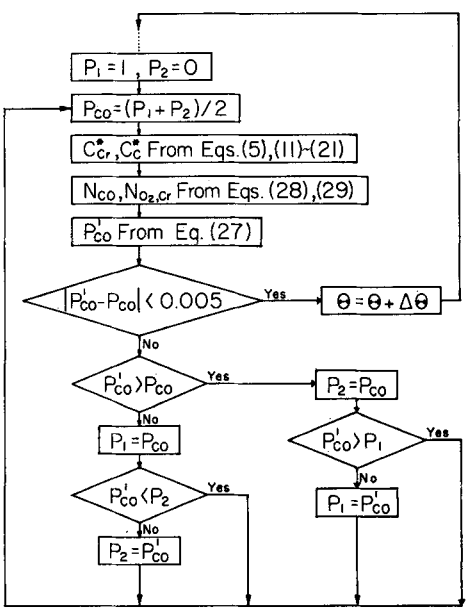

Fig. A1—Flow chart for estimating P_{CO}.

correspond to an accuracy of about 1 pct, the calculation would proceed to the next time step.

4) If the discrepancy between the two estimates was larger than 0.005 atm, then the difference was reduced by the following procedure:

The previously given limits on P_{CO}, viz. P_1 and P_2, were successively replaced by the previous estimates of P_{c0} depending on whether the quantity was positive or negative, as seen in Fig. A1.

This procedure had the advantage of stability and through the progressively narrowing interval that P_{co} could take, provided rapid convergence.

NOMENCLATURE

A	dimensionless number = $I\Theta_S$ (−)
a_j	activity of component j (pct j)
B	dimensionless number = $S\Theta_S/WC_S$
C_j	concentration of component j, (kg(j)/kg(Fe)), (pct)
C_S	standard concentration, (kg (j)/kg (Fe)), (pct)
c_j	dimensionless concentration of component $j = C_j/C_S$
e_j^i	interaction coefficient (1/j -pct)
f_j	activity coefficient (−)
I	conductances considered to incorporate all the resistances to transfer (1/s)
$K(T), K_1, K_2$	equilibrium constant [atm/((pct C) (pct O))] [1/((pct Cr)^2(pct O)^3)]
M_j	molecular weight of component j (kg/kg mol)
N_{co}	molar flow rate of CO due to decarburization (kg mol (co)/s kg (Fe))
N_{o_2}	flow rate of oxygen gas (kg mol (o_2)/s kg (Fe))
$N_{o_2,cr}$	molar flow rate of oxygen used for chromium oxidation (kg mol (o_2)/s kg (Fe))
P_t	total pressure of furnace atmosphere (atm)
P_{co}	partial pressure of carbon monoxide gas (atm)
S	feed rate of available oxygen (kg (O)/s)
T	temperature of molten steel (K)
W	mass of molten steel (kg)
α	stoichiometric coefficient (−)
λ	coefficient used in Eq. [27] (−)
Θ	elapsed time (sec)
Θ_S	standard time period (s)
θ	dimensionless elapsed time (−)

(Suffixes)

g	carrier gas
i	initial value
*	equilibrium state

ACKNOWLEDGMENTS

The authors wish to thank Dr. J. C. Fulton of Allegheny Ludlum Industries for helpful discussions and for drawing their attention to Refs. 4 and 5. Thanks are also due to the A. E. Anderson Foundation and to the National Science Foundation (Research Applied to National Needs) for support of this investigation.

REFERENCES

1. J. M. Saccomano, R. J. Choulet, and J. D. Ellis: *J. Metals*, vol. 21, February 1969, p. 59.
2. F. Oeters and K. Heyer: *Arch. Eisenhüttenw.*, 1959, vol. 5, p. 381.
3. Y. Niri, K. Ito, and K. Sano: *Testu-to-Hagane*, 1969, vol. 55, no. 6, p. 437.
4. L. F. Barnhardt: Ph.D. Thesis, 1965, MIT, Cambridge, Mass.
5. J. C. Fulton and S. Ramachandran: Proceedings of the Electric Steelmaking Conference, University Press, 1972.
6. T. Kuwano, S. Maruhashi, and Y. Aoyama: *Testu-to-Hagane*, 1973, vol. 59, no. 7, p. 863.
7. S. Asai and I. Muchi: *Testu-to-Hagane*, 1972, vol. 58, no. 6, p. 675.
8. S. Asai and I. Muchi: *Mathematical Modelling Techniques Relevant to the Iron and Steel Industry*, ISI, Delft, 22, February, 1973.
9. S. Asai and I. Muchi: *Trans. I.S.I.J.*, (in press).
10. S. Tamamoto, T. Ikeda, and K. Marukawa: *Tetsu-to-Hagane*, 1968, vol. 54, no. 2, p. 381.
11. K. Mori and H. Nomura: *Tetsu-to-Hagane*, 1970, vol. 55, no. 11, S 460.
12. K. Nakamura, T. Ohno, and K. Segawa: Proceedings of International Conference on the Science and Technology of Iron and Steel, 1970, vol. 1, p. 456.
13. J. Chipman: *J. Iron and Steel Inst.*, 1955, vol. 180, p. 97.